Controlled Disorder in Plant Light-Harvesting Complex II Explains Its Photoprotective Role

Tjaart P. J. Krüger,[†△] Cristian Ilioaia,[†△] Matthew P. Johnson,[‡] Alexander V. Ruban,[‡] Emmanouil Papagiannakis,[†] Peter Horton,[§] and Rienk van Grondelle[†*]

[†]Department of Physics and Astronomy, Faculty of Sciences, VU University Amsterdam, De Boelelaan, Amsterdam, The Netherlands; [‡]School of Biological and Chemical Sciences, Queen Mary University of London, London, United Kingdom; and [§]Department of Molecular Biology and Biotechnology, University of Sheffield, Sheffield, United Kingdom

ABSTRACT The light-harvesting antenna of photosystem II (PSII) has the ability to switch rapidly between a state of efficient light use and one in which excess excitation energy is harmlessly dissipated as heat, a process known as qE. We investigated the single-molecule fluorescence intermittency of the main component of the PSII antenna (LHCII) under conditions that mimic efficient use of light or qE, and we demonstrate that weakly fluorescing states are stabilized under qE conditions. Thus, we propose that qE is explained by biological control over the intrinsic dynamic disorder in the complex—the frequencies of switching establish whether the population of complexes is unquenched or quenched. Furthermore, the quenched states were accompanied by two distinct spectral signatures, suggesting more than one mechanism for energy dissipation in LHCII.

INTRODUCTION

Photosynthesis in plants is adapted to the continuous change in environmental conditions by the operation of various regulatory processes. One of these, nonphotochemical quenching of chlorophyll fluorescence, regulates the function of the light-harvesting antenna of photosystem II (PSII) (1). The rapidly reversible, energy-dependent component of nonphotochemical quenching, qE, protects the photosynthetic apparatus from overexcitation and ensuing photodamage by the harmless dissipation of excess excited states (1–3). The main component of the PSII antenna, the trimeric light-harvesting complex (LHCII), has been implicated as a major player in qE (1,4–7). Evidence suggests that more than one qE mechanism can coexist at different sites within the PSII antenna and prominent roles have been assigned not only to LHCII but also to the monomeric light-harvesting complex (LHC) CP29 (4,8).

LHCII is the major plant LHC, accounting for >50% of all land-bound chlorophyll. Each monomer of the LHCII trimer binds 14 chlorophylls (Chls), one neoxanthin (Neo) and two luteins (Luts). Violaxanthin (Vio) is a fourth, weakly bound xanthophyll (9) that via the enzymatic xanthophyll cycle is deepoxidized to zeaxanthin (Zea) in excess light (10). Under these excess light conditions, qE, triggered by the increase in the pH gradient across the thylakoid membrane (ΔpH), is enhanced by the action of the xanthophyll cycle (1). For CP29 the bound Zea has been proposed to be involved in qE (8), whereas for LHCII both Lut (7) and Zea (11) have been implicated. Spectroscopy of LHCII trimers in the quenched and unquenched state reveals differences in several bound pigments (1,6,7,12–14), indicating small, but specific changes in pigment-protein conformation upon the formation of the quenched state. Many of these spectroscopic features are also found in chloroplasts and leaves when qE is induced (7,15,16) and this strongly suggests that similar conformational changes are involved in the mechanism of qE in vivo.

All of these studies of quenched LHCII were performed on ensembles of molecules; samples were described as being unquenched or in various extents of quenching. Although quenching has been associated with conditions that induce protein aggregation (14,17), quenched states are also manifested in LHCII crystals (6) in which no strong intertrimeric interactions are present. In addition, quenching can be induced even when LHCII is immobilized in a gel matrix, in which protein aggregation is impossible (12). This strongly suggests that a single LHCII molecule has the inbuilt capacity to switch into a quenched state, i.e., the energy dissipation and the accompanying reversible conformational changes are very likely intrinsic features of each LHCII complex (6,12). Hence, it has been suggested that in vivo, under different light conditions, the size of the ΔpH and the deepoxidation state of the xanthophyll cycle determine the equilibrium between the different emissive states of LHCII, thereby establishing the extent of qE (18). However, such ensemble measurements, either in vitro or

Submitted March 1, 2012, and accepted for publication April 30, 2012.

△Tjaart P. J. Krüger and Cristian Ilioaia contributed equally to this work

*Correspondence: r.van.grondelle@vu.nl

Cristian Ilioaia's present address is Institute of Biology and Technology of Saclay, CEA, UMR 8221 CNRS, University Paris Sud, CEA Saclay, Gif sur Yvette, France.

Matthew P. Johnson's present address is Department of Molecular Biology and Biotechnology, University of Sheffield, Western Bank, Sheffield S10 2TN, UK.

Editor: Leonid Brown.

0006-3495/12/06/2669/8

doi: 10.1016/j.bpj.2012.04.044

in vivo, cannot adequately test such a hypothesis: it needs to be determined whether, in a light-harvesting sample, some complexes are in a quenched state and whether complexes in an unquenched state have the capacity to "visit" a dark state; i.e., whether the degree of quenching of an ensemble of LHCII complexes is determined by a dynamic equilibrium established by the frequencies of transfer between these states.

Recently, we applied single-molecule fluorescence spectroscopy to the study of quenching in LHCII. It was found that single LHCII trimers indeed exhibit dynamic fluorescence intensity and spectral fluctuations on timescales of milliseconds to tens of seconds (19,20). The intensity fluctuations occurred abruptly between various distinct levels, most frequently between strongly and weakly emitting states. This behavior appears to be common to a wide range of intrinsically fluorescent systems (21,22), pointing to substantial underlying dynamic disorder in these molecules. Furthermore, the sensitivity of the fluorescence intermittency from LHCII to the experimental conditions (23) suggests that the emissive state of LHCII can be modulated by its direct environment. The demonstration that LHCII has the inbuilt capacity to switch between spectroscopically and functionally different states (19,20,24) suggests that the exploitation and control of this inherent disorder could provide the molecular basis for qE.

Here, we directly tested this hypothesis by analyzing the changes in fluorescence intermittency from single LHCII trimers in different environments, in particular when an environment that mimics the in vivo conditions giving rise to efficient light harvesting was replaced with one mimicking the physiological conditions associated with qE.

MATERIALS AND METHODS

Sample preparation

The LHCII trimers that were enriched in Vio were isolated from photosystem-II particles prepared from thylakoids obtained from dark-adapted spinach leaves, as described previously (9). To prepare Zea-enriched trimers, the thylakoids were treated with 40 mM ascorbate at pH 5.5 before the isolation of the PSII particles (9). The two samples contained ~0.4–0.7 Vio and ~0.6 Zea per monomer, respectively (Table 1). Complexes were solubilized in 20 mM HEPES (pH 8), 1 mM $MgCl_2$, and 0.03% (w/v) *n*-dodecyl-β,D-maltoside [solution 1], diluted to a few pM, and attached onto a poly-L-lysine (Sigma, Schnelldorf, Germany) treated standard microscope coverslip. The solution that was flushed through the sample cell (25) before data acquisition determined the experimental environment: solution 1 mimicked the light-harvesting environment; addition of 15 mM sodium citrate to this solution facilitated stabilization of the pH at 5.5; and a detergent-free flushing solution was used to partially remove the micelles around attached trimers. Oxygen in the flushing solution was scavenged by the enzymatic system that comprised 200 μg/mL glucose oxidase, 7.5 mg/mL glucose, and 35 μg/mL catalase. Measurements were performed at 5°C. Complexes survived for typically ~1 min before photobleaching irreversibly.

Single-molecule spectroscopy

The experimental setup used to perform single-molecule confocal spectroscopy was described earlier (20,25). A continuous wave 632.8-nm helium-neon laser (JDS Uniphase, Eindhoven, The Netherlands) excitation source with an intensity of 250 W/cm^2 was used. The planar polarization of the light was changed into a near-circular state by a Berek polarization compensator (5540M; New Focus, Santa Clara, CA).

Data analysis

Data of fluorescence intensity and spectra were acquired in integration time bins of 10 ms and 1 s, respectively, and analyzed in MATLAB (The MathWorks, Natick, MA) as described before (19,20). The single-molecule, trimeric identity of the complexes was established by transitions into quenched or photobleached states that occurred within a single time step and by fluorescence intensities of unquenched states that corresponded well to the predicted value (23). As such, the data screening neglected intrinsically dim complexes. Second, complexes that survived shorter than one-third of the average survival time before irreversible photobleaching were neglected; because the corresponding intensity time traces produce artifactual changes in the power-law fitting parameters (see below). Third, complexes that exhibited an excessively large frequency of intensity fluctuations, which were often accompanied by relatively short survival times, were disregarded.

The weighted probability density of a dwell time τ was defined as (26) $P(\tau) = N(\tau)/(N_{tot}\ \Delta t_{ab})$, where the weighting factor $\Delta t_{ab} = (a+b)/2$. Here, $N(\tau)$ denotes the number of intensity levels with dwell time, N_{tot} is the total number of intensity levels, and a and b are the time differences between τ and the next longest and next shortest dwell times with nonzero probability, respectively. Power-law fits of the dwell time probability distributions were conducted, using a least mean-squares approximation of the function $P(\tau) \propto \tau^m$ for quenched intensities and $P(\tau) \propto \tau^m e^{-\tau/\tau_c}$ for unquenched intensities. Here, m denotes the power-law slope and τ_c the characteristic time after which an exponential behavior dominates the power-law behavior. The expectation value of a dwell time τ is defined as $\langle\tau\rangle = \sum P(\tau)\ \tau / \sum P(\tau)$.

TABLE 1 Pigment composition of isolated LHCII after sucrose gradient ultracentrifugation

LHCII	Neo	Vio	Ant	Lut	Zea	DEP	Chl *a*/*b*
Vio-enriched	27.0 ± 2.1 (1.09 ± 0.05)	10.3–18.0 ± 1.3 (0.40–0.70 ± 0.05)	0.0	55.0 ± 1.6 (2.2 ± 0.1)	0.0	0.0	1.3 ± 0.1
Zea-enriched	27.0 ± 1.2 (1.09 ± 0.05)	2.0 ± 0.2 (0.08 ± 0.01)	2.0 ± 0.2 (0.08 ± 0.01)	54.0 ± 2.2 (2.1 ± 0.1)	15.0 ± 2.1 (0.6 ± 0.1)	84.0	1.3 ± 0.1

Complexes isolated from photosystem-II-enriched particles (9) obtained from the thylakoids of dark-adapted plants (Vio-enriched) and by prior deepoxidation of the thylakoids at pH 5.5 in the presence of 40 mM ascorbate (Zea-enriched). Neo, Vio, Ant, Lut, Zea, DEP, Chl *a*/*b*: neoxanthin, violaxanthin, antheraxanthin, lutein, zeaxanthin, deepoxidation state and chlorophyll *a*/*b* ratio. Xanthophyll contents denote means and are expressed as a % of total xanthophyll ± SE from four replicates; DEP is (Zea + 0.5 Ant)/(Vio + Zea + Ant) (in %). Data in parentheses are the calculated xanthophyll contents per monomer of protein (molar ratio), assuming that one monomer has 14 Chls and a Chl/xanthophyll ratio of 3.5.

RESULTS AND DISCUSSION

Intensity switches

In our experiments the qE conditions were simulated by lowering the pH from 8.0 to 5.5 and partially removing the detergent micelles around single, immobilized, Zea-enriched complexes (see Table 1). A pH of 5.5 typically occurs in the intrathylakoid lumen in vivo under qE conditions; replacement of Vio with Zea mimics the xanthophyll cycle; and a low-detergent environment promotes a strong quenching in immobilized LHCII (when protein aggregation is prevented), which has many features that are similar to qE (12). Each of these three conditions was found to affect the behavior of LHCII under single-molecule conditions. In these experiments, we resolved the intensity fluctuations (Fig. S1 in the Supporting Material) by using an algorithm described previously (19) for sets of >100 individually measured LHCII trimers in different environments.

The histograms of these time-resolved intensities, portrayed in Fig. 1, *A* and *B*, consist of two broad peaks, the relative areas of which reflect the fractional dwell times in quenched and unquenched states, where "quenched" and "unquenched" refer to weakly and strongly fluorescing states, respectively. In general, every addition of a qE-related condition gave rise to an increase in the area of the "quenched" distribution and a decrease in the area of the "unquenched" distribution. The environmental effect on the peak intensities, the latter of which reflect the intrinsic brightness of the complexes, was less consistent.

To compare the intensity histograms with properties obtained for large ensembles of complexes, we calculated for each combination of the three qE-related conditions, the values of the average fluorescence intensity, $\bar{I}$, and the total dwell time in quenched states, $\sum\tau_Q$, as displayed in Fig. 1 *C*. The environmentally induced changes of these properties (Fig. 2, *A–F*), indicate that each of the qE-related conditions consistently resulted in an increase in $\sum\tau_Q$ and a decrease in $\bar{I}$. Qualitatively similar results were obtained when the individual intensity levels were not resolved but 10-ms binned intensities were used instead (Fig. S2).

Kinetic information of the switching between quenched and unquenched states is provided by the probability distribution of the dwell times in quenched (τ_Q) and unquenched (τ_{unQ}) states (Fig. 1, *D* and *E*). In this representation the slopes reflect the relative (in)stability of a quenched or an

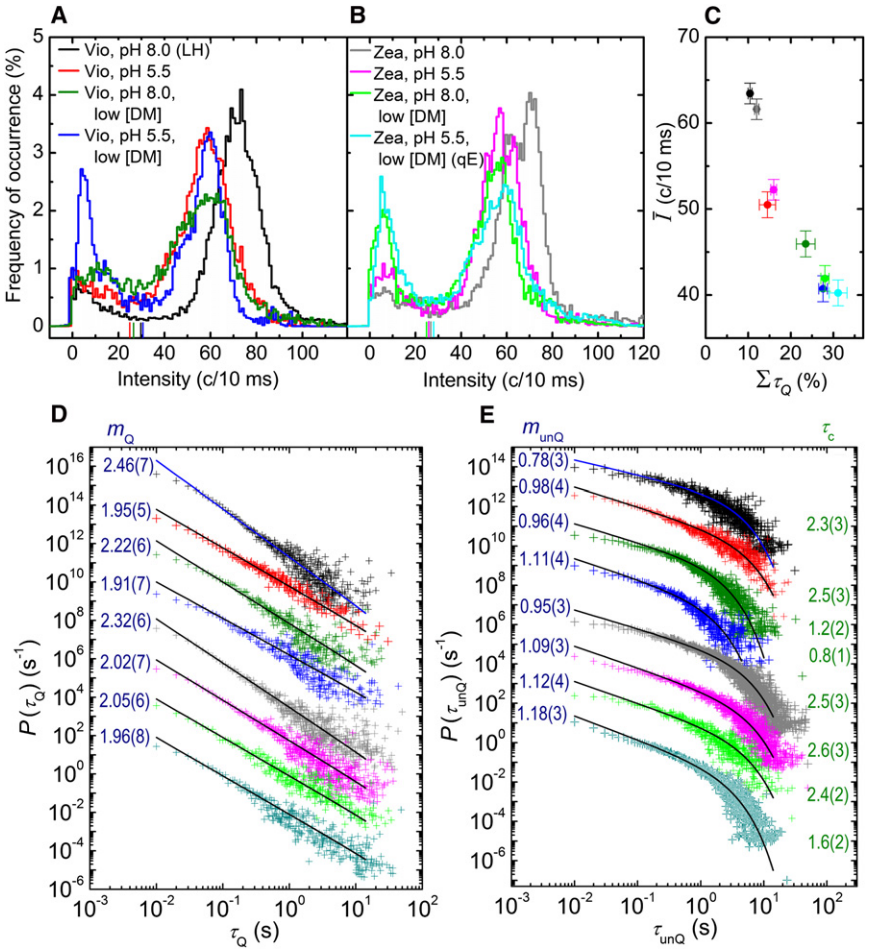

FIGURE 1 Properties of fluorescence intensity fluctuations of individually measured LHCII trimers exposed to different environments. (*A* and *B*) Intensity distributions in different environments, for intensity levels resolved as described in (19). Intensity bins of 1 count per 10 ms (c/10 ms) are indicated by horizontal steps of histograms. The thresholds between quenched and unquenched states are denoted by the short, vertical lines on the *x* axes and are defined as the intensity at which the histogram reaches a minimum between the broad quenched and unquenched histogram peaks. LH, light-harvesting mimicking state; qE, qE-mimicking state; low [DM], low detergent concentration. (*C*) Total dwell time in quenched states ($\sum\tau_Q$) and average intensity ($\bar{I}$) of distributions in Fig. 1, *A* and *B*, with matching colors. Error bars denote standard errors, including calibration uncertainties of absolute intensities. (*D* and *E*) Weighted probability distribution of dwell times in quenched (*D*) and unquenched (*E*) states in each environment (*crosses*) and least squares fits (*lines*). Fitting results of the power-law slopes in unquenched (m_{unQ}) and quenched (m_Q) are shown, together with the exponential cutoff time (τ_c). See Materials and Methods for details. Standard errors of fits are indicated in brackets. Deviations of fits at the shortest dwell times are apparent when intensity levels are resolved (see (19)). For clarity of display, data and fits are separated by factors of 10^2. The same data as for Fig. 1, *A* and *B*, were used.

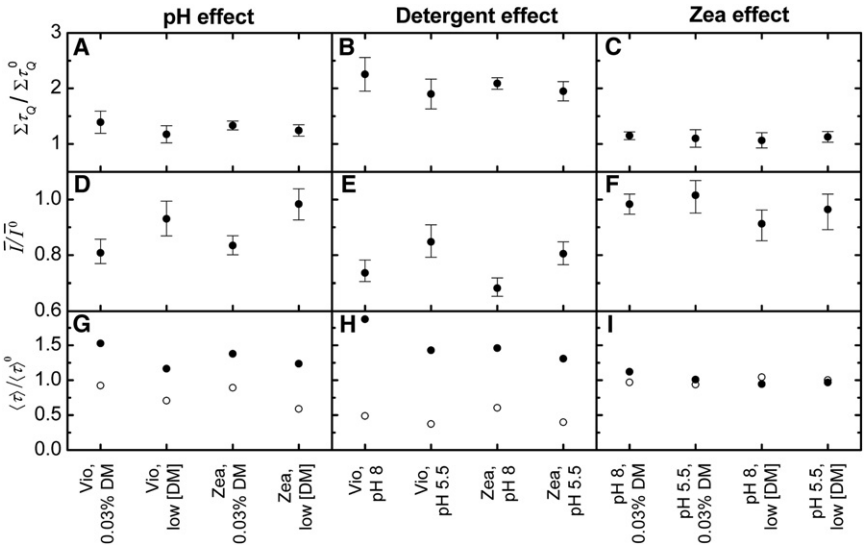

FIGURE 2 Effect of the three qE-related factors on the intensity dynamics of single LHCII trimers. (*A–C*) Fraction of increase in $\sum\tau_Q$ induced by the environment, where $\sum\tau_Q^0$ denotes the value before replacing the environment. *X* axes denote environmental conditions that remained constant. Error bars denote standard errors from Fig. 1 *C*. (*D–F*) Similar to Fig. 1, *D–F*, but for $\bar{I}$. (*G–I*) Similar to Fig. 1, *D–F*, but for the expectation value $\langle\tau\rangle$ of the dwell time in quenched (*solid circles*) and unquenched (*open circles*) states.

unquenched state: a steeper slope indicates that the relative abundance of short dwell times increased and thus that, on average, the associated quenched or unquenched states were destabilized. The presented slopes of the power-law fits show the overall trend of a decreasing m_Q (Fig. 1 *D*) and an increasing m_{unQ} (Fig. 1 *E*) as more qE-related conditions were added to the environment. Thus, in general, the qE-related conditions stabilized the quenched states and destabilized the unquenched states, i.e., both the probability to access a quenched state and the probability to dwell in this state for an extended time increased. Although this trend is apparent from the power-law slopes, it can be affected significantly by the frequency of fluctuations between quenched and unquenched states as well as the exponential cutoff times of the unquenched distribution (τ_c). To eliminate the possible ambiguity that results from the power-law approximation, the expectation values of the dwell times in quenched, $\langle\tau_Q\rangle$, and unquenched, $\langle\tau_{unQ}\rangle$, states were considered (Fig. 2, *G–I*). These values, which exclude data fitting of the dwell-time probability distributions while accounting for the effect of all the power-law parameters, confirmed the behavior revealed by the power-law slopes: virtually each of the qE-related conditions gave rise to an increase in $\langle\tau_Q\rangle$ and a decrease in $\langle\tau_{unQ}\rangle$.

Controlled disorder

The changes in $\sum\tau_Q$, $\bar{I}$, $\langle\tau_Q\rangle$, and $\langle\tau_{unQ}\rangle$ that were induced by altering the local pH, detergent, and xanthophyll epoxidation state imply that the intrinsic disorder that gives rise to fluorescence intermittency was modulated by each of these three conditions to favor energy dissipating states. Overall, the effect of qE conditions was less than that observed in ensemble measurements. This can at least partially be accounted for a), by the filtering criteria (see Materials and Methods), which neglected important factors such as the fraction of intrinsically dim complexes in any specific environment; b), by averaging over a large set of protein conformational states in an artificial environment; and c), by a possible detachment of some fraction of the weakly bound Vio or Zea during the course of the experiment. The Zea effect was the weakest and the detergent effect (protein solvation) the most significant, in agreement with previous ensemble measurements of LHCII quenching (1). The clear pH dependence shows that protons are one key factor in the modulation of fluorescence intermittency in these complexes, in agreement with the detailed investigation in (23). Any combination of the three qE-related conditions incurred a stronger quenching effect than the individual conditions, the most prominent effect occurring when all three were applied together, i.e., in the complete qE-mimicking environment. These findings strongly suggest a relationship between the mechanism(s) that underlie(s) fluorescence intermittency in these complexes and the transition involved in qE; i.e., the control over the intrinsic disorder in LHCII that gives rise to fluorescence intermittency is a possible molecular basis for the physiological regulation of the fate of excitation energy in these complexes.

Spectral properties

To obtain better insight into the properties of the quenched states, we investigated their corresponding spectral behavior (Fig. 3). Under light-harvesting conditions there was no relationship between transitions into quenched states and the observed red-shifted emission: no or only small spectral shifts were related to strongly quenched states. In contrast, large spectral shifts generally corresponded to a small degree of quenching, frequently even connected to superradiant states (Fig. 3 *A*). The spectral similarity of the quenched and unquenched states is supported by their

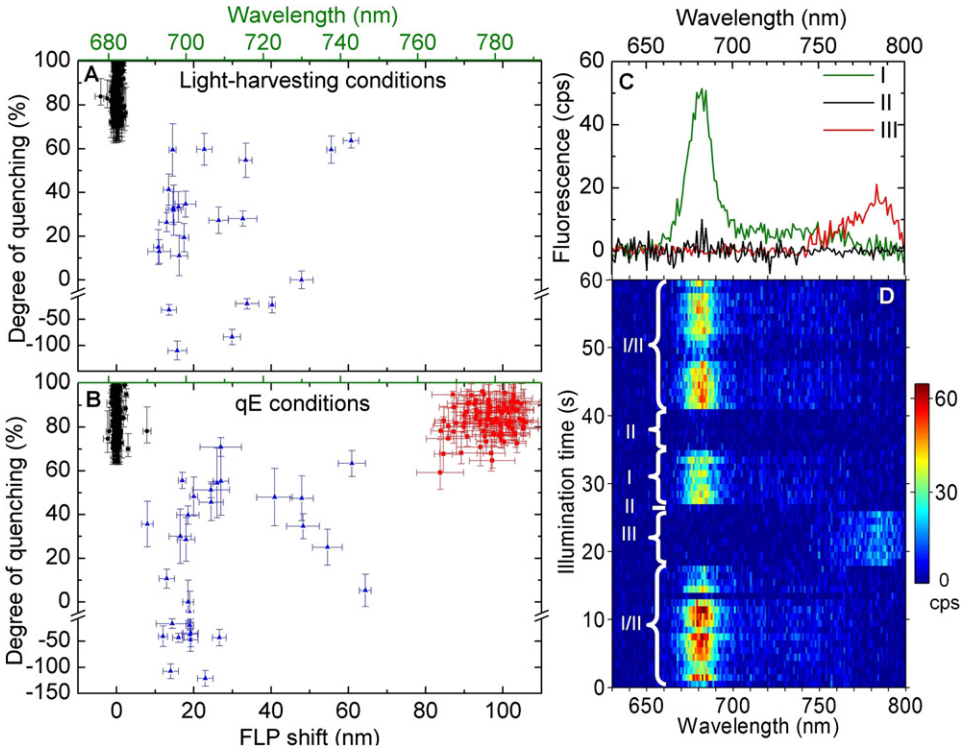

FIGURE 3 Spectral properties of the two types of energy-dissipating states. (*A* and *B*) Relationship between the degree of fluorescence quenching and shift in fluorescence peak position of ~400 individually measured LHCII trimers under light-harvesting (*A*) and qE (*B*) conditions. Black circles represent single-peak profiles corresponding to intensity decreases of at least 70%. Blue triangles signify the redder peaks of double-peak profiles. Error bars depict standard deviations (see the Supporting Material). Axis on top (*green*) indicates approximate peak position of the quenched state. (*C* and *D*) Example of spectral time trace under qE conditions where the two spectrally distinct types of quenched states are evident. Averages of "pure" states I, II, and III (*C*), e.g., state II corresponds to ~95% quenching and no fluorescence peak shift. I/II denotes alternation between states I and II (*D*). Intensities are expressed in counts/s (cps).

essentially identical spectral peak distributions (Fig. 4 *A*), the small discrepancy in the widths of which can be fully explained by the uncertainty in the resolved spectra. The lack of correlation between the peak wavelength and the extent of quenching in this spectral window implies that the absorbed energy can be quenched to different degrees, unrelated to the different spectral shapes, strongly suggesting that the red-shifted emission (~695–745 nm) from LHCII trimers involves a different origin than fluorescence intermittency. The absence of large spectral changes for the majority of switches into quenched states implies that the creation of the quenched state leaves the set of excitonic states of the chlorophylls in LHCII unaffected and thus must involve only a subtle conformational change. Note that the set of excitonic states depends sensitively on the distances and orientations of the transition dipoles of all the pigments in LHCII (27,28). Indeed, due to the high rigidity of the LHCII trimer (29), the speed and reversibility of intensity fluctuations between discrete levels, only small changes in the pigment-protein system are likely (30).

In the qE environment (Fig. 3 *B*) the relationship between intensity and spectral fluctuations below 750 nm was largely the same as for the light-harvesting conditions and can thus be explained in a similar manner as for Fig. 3 *A*. The negligible environmental effect in this spectral window is supported by the similarity of the spectral peak distributions of all emission states (Fig. 5) as well as those of the separate quenched and unquenched emission states (Fig. 4). Again, this suggests that the excitonic manifold of the majority of the quenched LHCII complexes is unchanged. Furthermore, the calculated spectral peak distribution (Fig. 5) indicates that the modeled disorder of the pigment site energies (20) fully accounts for the spectral shifts of profiles that peak below ~695 nm. In both environments the distribution of the experimental single-band spectral peaks was somewhat narrower than that of the calculated distribution. This suggests that the modeled disorder of the pigment site energies, which was obtained from analyzing the bulk spectral properties and excited state dynamics (20), may be an overestimation. The discrepancy may also be related to the restriction imposed on the protein's degrees of freedom due to the substrate binding. Although such an interaction with the substrate is expected to be sensitive to the utilized environmental changes, in particular the acidity, no spectral dependence on the local environment was observed.

Considering the full energy window, ~10% of the complexes in the qE environment exhibited a characteristic spectral band peaking at ~760–790 nm in correlation with a switch into a quenched state (Fig. 3 *B*); this band was generally observed for only a part of the measuring time (Fig. 3, *C* and *D*). Although a similar band was not observed under the utilized light-harvesting conditions at 5°C (Fig. 3 *A*), it appeared on a few occasions under similar conditions but at elevated temperatures (Fig. S3). This indicates that the far-red states are not specifically dependent on the qE environment but have a much higher probability to be accessed than under light-harvesting conditions.

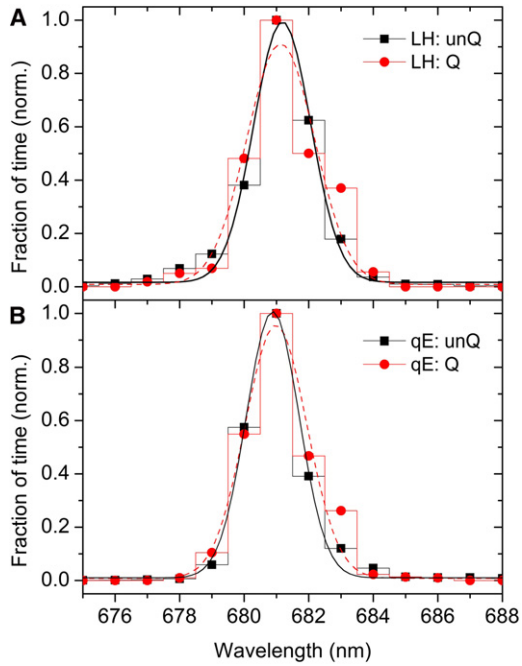

FIGURE 4 Fluorescence peak distributions of unquenched (*black squares*) and quenched (*gray circles*, *red online*) states of single LHCII complexes in the light-harvesting (*A*) and qE (*B*) environments. Horizontal steps indicate the bin size. Dashed lines denote color-coded Gaussian fits. In both conditions, the quenched peak distribution is ~9% broader than the unquenched distribution.

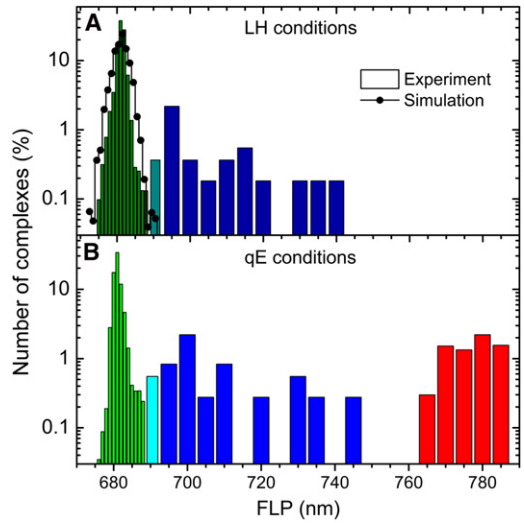

FIGURE 5 Spectral peak distributions of single LHCII trimers in two different environments. (*A*) Histogram in light-harvesting environment (*bars*) as compared to the modeled distribution (*points connected by lines*). Calculations were performed by a disordered-exciton–Redfield model, based on the modeling of ensemble spectroscopic data (37); 2000 realizations of the static disorder for a disorder of 90 cm^{-1} were used. Dark blue bars indicate spectral states that were not reproduced by the calculations and the light blue bar signifies a "transition region". Bins of 1 and 5 nm were used for the green and blue bars, respectively. Green bars denote the weighted frequency of occurrence of single-band spectral peaks, whereas the blue bars represent the fraction of complexes exhibiting double-band spectra, where the peak position of the redder band is displayed. The full width at half-maximum of a Gaussian fit to the green and calculated distribution is 2.1 nm and 4.2 nm, respectively. Resolved spectra of both quenched and unquenched states are included. (*B*) Similar to *A* but for the qE environment. A Gaussian fit of the green distribution has a full width at half-maximum of 1.9 nm.

Two qE mechanisms

The two distinct spectral signatures that accompanied the formation of quenched states, emission peaking at ~682 nm and ~760–790 nm, respectively, point to at least two different mechanisms of quenching in these complexes, both of which may be related to a distinct mechanism of qE. We propose that both mechanisms underlying fluorescence intermittency originate from Lut-Chl coupling in the Lut1 site, with the primary mechanism involving energy transfer from a Chl singlet state to the Lut S_1 state (7) and the secondary mechanism employing mixing of a charge-transfer state of this Lut with an excitonic state of the ensemble of Chls in this site. Additionally, the red-shifted double-band emission spectra below 750 nm observed under light-harvesting conditions have previously been suggested to originate from a Chl-Chl excitonic charge-transfer interaction in the Lut2 site (20), in accordance with the conclusion that these spectral features originate from a site other than that of fluorescence intermittency.

Recently, the presence of two distinct qE mechanisms in LHCII was confirmed by Stark fluorescence spectroscopy (31). The associated red-shifted emission, peaking at 696 nm and 713–715 nm, was tentatively assigned to excitonic charge-transfer mixing of Chl-Chl and Car-Chl ensembles, respectively. The latter mechanism, which was suggested to involve Lut1, might be related to the far-red quenched states (with emission peaking at ~760–790 nm) identified under our single-molecule conditions, considering that the energetically sensitive charge-transfer states could be altered significantly under the applied single-molecule conditions. Alternatively, the red-shifted states emitting below ~745 nm might be related to both mechanisms proposed in (31), in which case the quenching properties might be largely suppressed under the utilized single-molecule conditions.

Conformational nanoswitch

The reversibility of all of the observed transitions suggests that the different LHCII states are not artifactual but rather physiological states that may also be populated in vivo. Thus, LHCII is revealed as a natural conformational nanoswitch that regulates the transfer or emission of absorbed energy by rapidly and reversibly changing between unquenched and quenched energy states. We have demonstrated that LHCII has the inbuilt capacity to adopt four distinct conformational states, namely, two unquenched and two quenched states (Fig. 6). One quenched state and

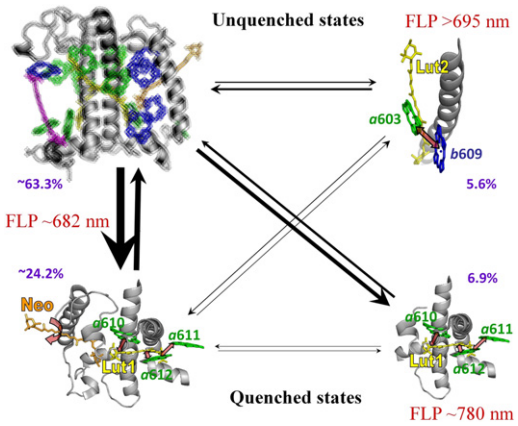

FIGURE 6 Model illustrating the molecular mechanism of the switches to red-shifted and two types of energy-dissipating states. LHCII monomeric structure (38) in an unquenched state, exhibiting emission at ~682 nm (*top left*). The induced uncertainty in the molecular positions indicates the subtle structural difference in the unquenched structure as compared to the resolved quenched structure. Key pigments involved in the establishment of the unquenched, red-shifted states (20) (*top right*), spectrally nonshifted, quenched states (7) (*bottom left*), and spectrally shifted, quenched states (*bottom right*). Straight, red arrows signify strong interactions; curved arrow indicates a configurational twist; black arrows represent transitions between different states, with the thickness giving a qualitative indication of the frequency of occurrence. Percentages in purple denote total dwell time in each state under qE conditions. See text for details.

one unquenched state are characterized by red-shifted fluorescence, where the red-shifted, quenched state becomes accessible primarily under qE conditions. Switching between all the states is rapid and reversible. We propose that a subtle perturbation in the physicochemical environment shifts the equilibrium to favor the quenched states. Thus, in vivo, associations with neighboring LHCII molecules in the ordered arrays of LHCII-PSII supercomplexes of the thylakoid membrane and the absence of Zea are envisaged to stabilize the unquenched states, whereas interaction with PsbS (32), protonation, aggregation (33), and Zea binding (10) would shift the equilibrium to favor the quenched states (18,34), though the precise details of this shift may differ from the utilized in vitro situation.

CONCLUSIONS

We have shown that LHCII has a dynamic function that does not depend on a large conformational switch between different states but rather on subtle changes in pigment configurations and/or environmental changes that originate from the intrinsic disorder of these complexes that allows them to switch between emissive and dark states. This intrinsic disorder enables the protein in each monomer to access numerous energetically similar substates of its energy landscape (35), with some of those substates having very different emission properties as a consequence of the ordering of their excited states; e.g., a fluorescent state has the carotenoid S_1 level above the lowest exciton state, whereas a quenched state has the carotenoid S_1 below the lowest exciton state. In the case of qE, plants exploit and control this disorder-specific coordinate of their energy landscape to provide a highly sensitive and effective regulatory mechanism important to their capability to use solar energy in photosynthesis. Disorder is common in protein systems and, for example, may play a significant role in enzymatic reactions in the context of the so-called conformational selection or population-shift model (36). Thus, it is likely that the exploitation of a system's intrinsic disorder to shift the population equilibrium, and hence the protein function, will be found in other biologically important processes.

SUPPORTING MATERIAL

Supporting Figs. S1, S2, and S3, a description of the data analysis performed for Fig. 3 in the main text, and supporting references are available at http://www.biophysj.org/biophysj/supplemental/S0006-3495(12)00518-8.

This work was supported by the EU FP6 Marie Curie Early Stage Training Network via the Advanced Training in Laser Sciences project (T.P.J.K.); the EU FP7 Marie Curie Reintegration Grant (C.I.); research and equipment grants from UK Biological Sciences Research Council and Engineering and Physical Science Research Council (EPSRC) (M.P.J. and A.V.R.); VENI grant from the Netherlands Organization for Scientific Research (NWO) (E.P.); Project Sunshine, University of Sheffield (P.H.); TOP grant (700.58.305) from the Foundation of Chemical Sciences, part of the NWO (T.P.J.K. and R.v.G.), and the Advanced Investigator Grant (267333, PHOTPROT) from the European Research Council (T.P.J.K. and R.v.G.).

REFERENCES

1. Horton, P., A. V. Ruban, and R. G. Walters. 1996. Regulation of light harvesting in green plants. *Annu. Rev. Plant Physiol. Plant Mol. Biol.* 47:655–684.
2. Niyogi, K. K. 1999. Photoprotection revisited: genetic and molecular approaches. *Annu. Rev. Plant Physiol. Plant Mol. Biol.* 50:333–359.
3. Ruban, A. V., M. P. Johnson, and C. D. Duffy. 2012. The photoprotective molecular switch in the photosystem II antenna. *Biochim. Biophys. Acta.* 1817:167–181.
4. Holzwarth, A. R., Y. Miloslavina, …, P. Jahns. 2009. Identification of two quenching sites active in the regulation of photosynthetic light-harvesting studied by time-resolved fluorescence. *Chem. Phys. Lett.* 483:262–267.
5. Müller, M. G., P. Lambrev, …, A. R. Holzwarth. 2010. Singlet energy dissipation in the photosystem II light-harvesting complex does not involve energy transfer to carotenoids. *ChemPhysChem.* 11:1289–1296.
6. Pascal, A. A., Z. F. Liu, …, A. Ruban. 2005. Molecular basis of photoprotection and control of photosynthetic light-harvesting. *Nature.* 436:134–137.
7. Ruban, A. V., R. Berera, …, R. van Grondelle. 2007. Identification of a mechanism of photoprotective energy dissipation in higher plants. *Nature.* 450:575–578.
8. Ahn, T. K., T. J. Avenson, …, G. R. Fleming. 2008. Architecture of a charge-transfer state regulating light harvesting in a plant antenna protein. *Science.* 320:794–797.
9. Ruban, A. V., P. J. Lee, …, P. Horton. 1999. Determination of the stoichiometry and strength of binding of xanthophylls to the photosystem II light harvesting complexes. *J. Biol. Chem.* 274:10458–10465.

10. Demmig-Adams, B., W. W. Adams, …, O. Björkman. 1990. Inhibition of zeaxanthin formation and of rapid changes in radiationless energy dissipation by dithiothreitol in spinach leaves and chloroplasts. *Plant Physiol.* 92:293–301.

11. Standfuss, J., A. C. Terwisscha van Scheltinga, …, W. Kühlbrandt. 2005. Mechanisms of photoprotection and nonphotochemical quenching in pea light-harvesting complex at 2.5 A resolution. *EMBO J.* 24:919–928.

12. Ilioaia, C., M. P. Johnson, …, A. V. Ruban. 2008. Induction of efficient energy dissipation in the isolated light-harvesting complex of Photosystem II in the absence of protein aggregation. *J. Biol. Chem.* 283:29505–29512.

13. Liao, P. N., C. P. Holleboom, …, P. J. Walla. 2010. Correlation of Car S(1) → Chl with Chl → Car S(1) energy transfer supports the excitonic model in quenched light harvesting complex II. *J. Phys. Chem. B.* 114:15650–15655.

14. Mullet, J. E., and C. J. Arntzen. 1980. Simulation of grana stacking in a model membrane system. Mediation by a purified light-harvesting pigment-protein complex from chloroplasts. *Biochim. Biophys. Acta.* 589:100–117.

15. Bode, S., C. C. Quentmeier, …, P. J. Walla. 2009. On the regulation of photosynthesis by excitonic interactions between carotenoids and chlorophylls. *Proc. Natl. Acad. Sci. USA.* 106:12311–12316.

16. Johnson, M. P., and A. V. Ruban. 2009. Photoprotective energy dissipation in higher plants involves alteration of the excited state energy of the emitting chlorophyll(s) in the light harvesting antenna II (LHCII). *J. Biol. Chem.* 284:23592–23601.

17. Ruban, A. V., and P. Horton. 1992. Mechanism of delta-pH-dependent dissipation of absorbed excitation-energy by photosynthetic membranes. 1. Spectroscopic analysis of isolated light-harvesting complexes. *Biochim. Biophys. Acta.* 1102:30–38.

18. Horton, P., M. P. Johnson, …, A. V. Ruban. 2008. Photosynthetic acclimation: does the dynamic structure and macro-organisation of photosystem II in higher plant grana membranes regulate light harvesting states? *FEBS J.* 275:1069–1079.

19. Krüger, T. P. J., C. Ilioaia, and R. van Grondelle. 2011. Fluorescence intermittency from the main plant light-harvesting complex: resolving shifts between intensity levels. *J. Phys. Chem. B.* 115:5071–5082.

20. Krüger, T. P. J., V. I. Novoderezhkin, …, R. van Grondelle. 2010. Fluorescence spectral dynamics of single LHCII trimers. *Biophys. J.* 98:3093–3101.

21. Cichos, F., C. von Borczyskowski, and M. Orrit. 2007. Power-law intermittency of single emitters. *Curr. Opin. Colloid Interface Sci.* 12:272–284.

22. Kulzer, F., and M. Orrit. 2004. Single-molecule optics. *Annu. Rev. Phys. Chem.* 55:585–611.

23. Krüger, T. P. J., C. Ilioaia, …, R. van Grondelle. 2011. Fluorescence intermittency from the main plant light-harvesting complex: sensitivity to the local environment. *J. Phys. Chem. B.* 115:5083–5095.

24. Krüger, T. P. J., E. Wientjes, …, R. van Grondelle. 2011. Conformational switching explains the intrinsic multifunctionality of plant light-harvesting complexes. *Proc. Natl. Acad. Sci. USA.* 108:13516–13521.

25. Rutkauskas, D., V. Novoderezkhin, …, R. van Grondelle. 2004. Fluorescence spectral fluctuations of single LH2 complexes from *Rhodopseudomonas acidophila* strain 10050. *Biochemistry.* 43:4431–4438.

26. Kuno, M., D. P. Fromm, …, D. J. Nesbitt. 2001. "On"/"off" fluorescence intermittency of single semiconductor quantum dots. *J. Chem. Phys.* 115:1028–1040.

27. Novoderezhkin, V., A. Marin, and R. van Grondelle. 2011. Intra- and inter-monomeric transfers in the light harvesting LHCII complex: the Redfield-Förster picture. *Phys. Chem. Chem. Phys.* 13:17093–17103.

28. van Grondelle, R., and V. I. Novoderezhkin. 2006. Energy transfer in photosynthesis: experimental insights and quantitative models. *Phys. Chem. Chem. Phys.* 8:793–807.

29. Barros, T., A. Royant, …, W. Kühlbrandt. 2009. Crystal structure of plant light-harvesting complex shows the active, energy-transmitting state. *EMBO J.* 28:298–306.

30. van Oort, B., A. van Hoek, …, H. van Amerongen. 2007. Equilibrium between quenched and nonquenched conformations of the major plant light-harvesting complex studied with high-pressure time-resolved fluorescence. *J. Phys. Chem. B.* 111:7631–7637.

31. Wahadoszamen, M., R. Berera, …, R. van Grondelle. 2012. Identification of two emitting sites in the dissipative state of the major light harvesting antenna. *Phys. Chem. Chem. Phys.* 14:759–766.

32. Li, X. P., O. Björkman, …, K. K. Niyogi. 2000. A pigment-binding protein essential for regulation of photosynthetic light harvesting. *Nature.* 403:391–395.

33. Johnson, M. P., T. K. Goral, …, A. V. Ruban. 2011. Photoprotective energy dissipation involves the reorganization of photosystem II light-harvesting complexes in the grana membranes of spinach chloroplasts. *Plant Cell.* 23:1468–1479.

34. Kereïche, S., A. Z. Kiss, …, P. Horton. 2010. The PsbS protein controls the macro-organisation of photosystem II complexes in the grana membranes of higher plant chloroplasts. *FEBS Lett.* 584:759–764.

35. Frauenfelder, H., S. G. Sligar, and P. G. Wolynes. 1991. The energy landscapes and motions of proteins. *Science.* 254:1598–1603.

36. Tsai, C. J., S. Kumar, …, R. Nussinov. 1999. Folding funnels, binding funnels, and protein function. *Protein Sci.* 8:1181–1190.

37. Novoderezhkin, V. I., M. A. Palacios, …, R. van Grondelle. 2004. Energy-transfer dynamics in the LHCII complex of higher plants: modified redfield approach. *J. Phys. Chem. B.* 108:10363–10375.

38. Liu, Z., H. Yan, …, W. Chang. 2004. Crystal structure of spinach major light-harvesting complex at 2.72 A resolution. *Nature.* 428: 287–292.